

Disturbance Observer Based Control for an Underwater Biomimetic Vehicle-Manipulator System with Mismatched Disturbances

Jiaqi Lv^{1,2}, Yu Wang^{*2}, Shuo Wang^{1,2,3}, Rui Wang², Long Cheng^{1,2}, and Min Tan^{1,2}

1. School of Artificial Intelligence, University of Chinese Academy of Sciences, Beijing 100049, P. R. China

2. Institute of Automation, Chinese Academy of Sciences, Beijing 100190, P. R. China

3. CAS Center for Excellence in Brain Science and Intelligence Technology, Shanghai 200031, P. R. China

Abstract: In this paper, a disturbance observer based control (DOBC) framework is proposed to achieve the motion control of an underwater biomimetic vehicle-manipulator system (UBVMS) driven by bionic flippers with mismatched disturbances. First, a disturbance observer is established to estimate the mismatched disturbances in finite time. Then, a novel arctangent non-singularity sliding mode manifold incorporating the disturbance observer is proposed to counteract the lumped mismatched disturbances. The stability of the system is validated by the Lyapunov theory. Finally, various comparative simulations are carried out to validate the performance of our proposed DOBC framework in the presence of mismatched disturbances.

Key Words: Underwater biomimetic vehicle-manipulator system (UBVMS), disturbance observer, arctangent non-singularity sliding mode controller (ANTSMC), mismatched disturbances.

1 Introduction

Nowadays, with the research and exploration of the marine field, underwater vehicle-manipulator systems (UVMSs) which are powered by thrusters play a critical role in ocean exploration tasks, such as underwater welding, marine intervention missions, and so on [1]. The earlier UVMS which could operate tasks was designed in Semi Autonomous Underwater Vehicle for Intervention Mission (SAUVIM) project by the University of Hawaii [2], which was tested by target recovery experiments in real shallow water. In the European Union project, GIRONA500 [3] realized the turn valve application under the autonomous floating-base condition. Japanese researchers developed an UVMS called KAIKO [4], which had good performances of the automatic navigation control. In real ocean experiments, KAIKO could cut ferromanganese crust and deposited them in a sample basket. In the Italian marine robotics for interventions (MARIS) project, Casalino *et al.* [5] designed an UVMS named R2, which could grasp a pipe in a pool environment.

However, with the development of bionics, underwater biomimetic robots have aroused great interest of researchers due to their high mobility and stability. Furthermore, underwater robots in bionic propulsion mode can avoid the disadvantage of thrusters being entangled by water plants. Zhang *et al.* [6] designed a robotic fish composed of insect wings and fins to achieve high mobility. Li *et al.* [7] designed a two-link robotic fish, and a P-type iterative learning control was proposed to achieve the precise speed control. Säulumae *et al.* [8] designed an underwater biomimetic robot with four

This work was supported in part by the National Key Research and Development Program of China under Grant 2020YFC1512202, in part by the Youth Innovation Promotion Association CAS under Grant 2018162, in part by the National Natural Science Foundation of China under Grant U1713222, Grant 62073316, Grant U1806204, 62033013, in part by key projects of foreign cooperation of CAS under Grant 173211KYSB20200020, in part by the Strategic Priority Research Program of Chinese Academy of Science, Grant No. XDB32050100.

*Corresponding author: Yu Wang (email: yu.wang@ia.ac.cn).

fins. The modular control method was used to decrease the errors of motion tracking and was validated by underwater experiments. Wang *et al.* [9] designed a robot driven by ribbon-fins, and the path following was achieved by a backstepping method in a swimming pool.

Besides, in the water, the stability of underwater biomimetic vehicles is often affected by disturbances. Some of them are mismatched disturbances, which means they exist in different channels rather than the control input channel. It should be pointed out that mismatched disturbances are very common in practical systems, and they can affect system states directly. Various control strategies are proposed to address the problem of mismatched disturbances. However, the mismatched disturbances should satisfy the H_2 norm-bounded. Another approach to address mismatched disturbances interference is to design disturbance observer-based control (DOBC) frameworks. Ginoya *et al.* [10] proposed an extended disturbance observer for a general n th order mismatched disturbance, and a modified sliding mode surface was proposed to counteract the disturbance. Zhang *et al.* [11] proposed a steady-state output-based strategy to design disturbance rejection gains, and the experiment of stabilizing a ball on the smooth beam verified the performance. Huang *et al.* [12] proposed a high-order disturbance observer for robotic systems, and the gain matrix of the observer was obtained through a linear matrix inequality method. Simulations verified the efficiency of the proposed DOBC method. Min *et al.* [13] proposed a composite controller based on a disturbance observer and a finite time backstepping method for robots, and the stronger stability was validated simulations. Yang *et al.* [14] proposed a DOBC method for a MAGLEV suspension system. The simulation demonstrated the better performance of the MAGLEV when meeting high-order mismatched disturbances.

Nevertheless, the above-mentioned researches were hardly designed a DOBC method for underwater vehicles to resist mismatched disturbances, and most observers could not converge in finite time. Hence, taking into account

the advantages of bionic robots, an underwater biomimetic vehicle-manipulator system (UBVMS) mechanical model with four flippers is designed and introduced in detail. Then, a DOBC framework composed of a novel arctangent non-singularity sliding mode controller (ANTSMC) and a disturbance observer with finite time convergence is proposed to realize motion control of the UBVMS in the presence of mismatched disturbances. Finally, comparative simulations are carried out to validate the performances of the proposed DOBC framework.

The remainder of this article is organized as follows. The mechanical structure and dynamics model of the UBVMS is described in Section II. Section III gives the design of the DOBC framework, and simulation results of the UBVMS resisting mismatched disturbances are given in Section IV. Section V gives the conclusion.

2 Mechanical Structure and Dynamics of the UB-VMS

2.1 Mechanical Structure of the UBVMS

The mechanical design of the UBVMS is based on modular design concepts. It consists of a control cabin, a visual process cabin, a 4 degree-of-freedom (4-DOF) underwater manipulator, and four bionic flippers. The details of the schematic representation are shown in Fig. 1. The control cabin is placed at the rear of the UBVMS and integrated many electronic devices. It is equipped with a power supply module, a network switch, a microcontroller, and so on. The control cabin is responsible for the program processing and returns/receives data to the upper control center.

The visual process system, which is arranged at the front of the body to balance the weight of the rear, is equipped with two pairs of binocular cameras and a process cabin. The 4-DOF manipulator is a lightweight manipulator which is made of nylon plastic. Four bionic flippers are located at the corners to generate the horizontal thrust. The flippers are driven by maxon motors and drivers, as shown in Fig. 1. The UBVMS can produce different motion modes by adjusting the initial phase, flapping angles, and frequencies of the bionic flippers.

2.2 Dynamics of the UBVMS

Two coordinates, namely earth-fixed reference frame O_{E-XYZ} and body-fixed frame O_{B-XYZ} , are shown in Fig. 1. Given the good stability of the UBVMS, neglecting the change of roll and pitch angles is reasonable (i.e., $\phi = 0$, $\theta = 0$). Then, we use a general modeling method of rigid to establish the dynamic model of the UBVMS [15], the dynamic model equation for the UBVMS can be written in the body-fixed frame as follows:

$$M\dot{\nu} + C(\nu)\nu + D\nu = \tau, \quad (1)$$

$$\nu = [u \ v \ r]^T, \quad (2)$$

where M is the inertia matrix including hydrodynamic added inertia, $C(\nu)$ is the coriolis and centripetal matrix, D is the damping matrix, τ is the thrust of the flippers, τ_d is the total mismatched disturbances. And u, v represent the surge and sway velocity, r represents the yaw angular velocity. The transition from the body-fixed frame to the earth-fixed frame

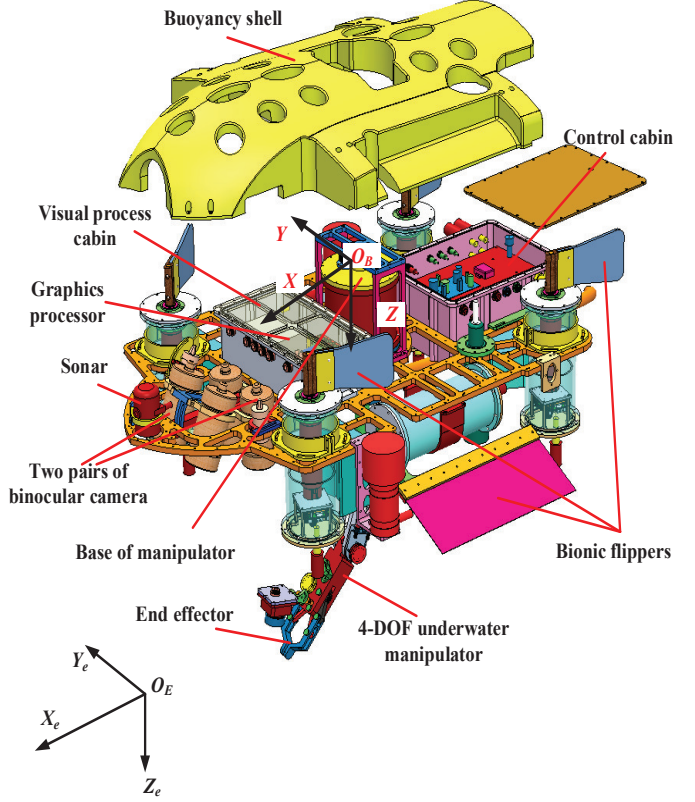


Fig. 1: Overview of the UBVMS.

is given:

$$\dot{\eta} = J(\eta)\nu \quad (3)$$

where the vector $\eta \in \mathbb{R}^{3 \times 3}$ denotes the positions and yaw angle in the earth-fixed frame, the matrix $J(\eta)$ denotes the rotational transform matrix. We can get the UBVMS dynamic model with total disturbance represented in the earth-fixed frame:

$$\begin{cases} \dot{u} = \frac{1}{m_1}(m_2v\psi - d_1u + \tau_u) \\ \dot{v} = \frac{1}{m_2}(-m_1u\dot{\psi} - d_2v + \tau_v) \\ \ddot{\psi} = \frac{1}{m_6}(-m_2vu + m_1uv - d_6\dot{\psi} + \tau_\psi) \\ \dot{x} = u\cos(\psi) - v\sin(\psi) \\ \dot{y} = u\sin(\psi) + v\cos(\psi), \end{cases} \quad (4)$$

among them, x, y, z denote the position and ψ denotes the yaw angle in earth-frame respectively, the control inputs are represented as:

$$\begin{cases} F_i = fal(\sigma_i) \\ \sigma_i = A_i \sin(2\pi f_i t + \phi_i) + \theta_i, \end{cases} \quad (5)$$

among them, σ_i is the actual flipping angle, A_i is the magnitude, f_i is the frequency, ϕ_i is the phase of the i -th flipper respectively. fal is a nonlinear mapping function between the actual angle σ_i generated by i -th flipper and the thrust F_i , which is obtained through the real experimental testing. So far, we have established the dynamic model of the UBVMS.

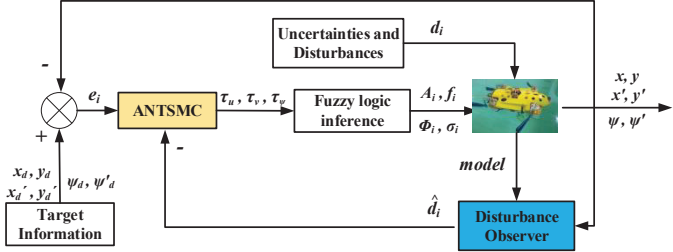


Fig. 2: Block diagram of the DOBC framework.

3 DOBC Framework Design

In this section, a new DOBC control scheme which consists of ANTSMC and mismatched disturbance observer is designed. The ANTSMC has high robustness and makes system states convergence to the desired position faster than conventional non-singularity sliding mode controller (NTSMC). Considered to compensate for mismatched disturbances, a finite-time observer for mismatched disturbances of the UBVMS is firstly introduced.

3.1 Disturbance Observer with Finite Time Convergence

The mismatched disturbances caused by unmodeled dynamics and parameter perturbations of the UBVMS can affect the system states directly. We use the dynamic model of the UBVMS with mismatched disturbances in the earth-fixed frame to design the observer. The dynamics are given:

$$\begin{cases} \dot{x}_{1i} = \nu + d_i \\ = [u \ v \ r]^T \\ \dot{x}_{2i} = f(\nu) + \tau_M \\ f(\nu) = -M^{-1}[C(\nu)\nu + D\nu] \\ \tau_M = M^{-1}\tau, \end{cases} \quad (6)$$

where, x_{1i} is the disturbed system state, d_i is mismatched disturbance acting on the system state. A finite-time observer for the mismatched disturbance d_i of the UBVMS is firstly introduced:

$$\begin{cases} \dot{z}_{0i} = v_{0i} + \nu \\ v_{0i} = -\lambda_0|z_{0i} - x_{1i}|^{2/3}sign(z_{0i} - x_{1i}) + z_{1i} \\ \dot{z}_{1i} = v_{1i}, v_{1i} = -\lambda_1|z_{1i} - v_{0i}|^{1/2}sign(z_{1i} - v_{0i}) + z_{2i} \\ \dot{z}_{2i} = v_{2i}, v_{2i} = -\lambda_2sign(z_{2i} - v_{1i}), \end{cases} \quad (7)$$

where $\lambda_i > 0$ are the observer gains to be designed, and z_1 is the estimation \hat{d}_i , z_2 is the estimation $\dot{\hat{d}}_i$. Define $\epsilon_0 = z_0 - x_{1i}$, $\epsilon_1 = z_1 - d_i$, $\epsilon_2 = z_2 - \dot{d}_i$, we can obtain:

$$\begin{cases} \dot{\epsilon}_0 = -\lambda_0|\epsilon_0|^{2/3}sign(\epsilon_0) + \epsilon_1 \\ \dot{\epsilon}_1 = -\lambda_1|\epsilon_1 - \dot{\epsilon}_0|^{1/2}sign(\epsilon_1 - \dot{\epsilon}_0) + \epsilon_2 \\ \dot{\epsilon}_2 = -\lambda_2|\epsilon_2 - \dot{\epsilon}_1|sign(\epsilon_2 - \dot{\epsilon}_1) - \ddot{d}_i, \end{cases} \quad (8)$$

it follows from [16] that the estimation errors ϵ_i ($i = 1, 2, 3$) are finite time stable, which means that $\epsilon_i(t) = 0$.

3.2 Improved ANTSMC for the UBVMS

Define

$$\begin{cases} e_{1i} = x_{di} - x_{1i} \\ e_{2i} = \dot{x}_{di} - x_{2i}, \end{cases} \quad (9)$$

we can obtain $\dot{e}_{1i} = e_{2i} - d_i$. Then, an improved ANTSMC is proposed for the UBVMS under the mismatched disturbances, the sliding mode manifold is designed as follow:

$$s = \frac{1}{\beta}(e_{2i} - \hat{d}_i)^{p/q} + (1 + e_{1i}^2)^{p/q}arctan(e_{1i}), \quad (10)$$

where p, q are positive odds and satisfy $1 < p/q < 2$, β is a positive constant. For the system (7) and sliding mode manifold (10), the control law is designed as:

$$\begin{aligned} \tau_M = & \frac{\beta q}{p}(e_{2i} - \hat{d}_i)^{2-\frac{p}{q}}(1 + e_{1i}^2)^{\frac{p}{q}-1}[1 + \frac{2p}{q}e_{1i}arctan(e_{1i})] \\ & + \ddot{x}_d - f(\nu) - \dot{\hat{d}}_i + k_i s + eta_i \cdot sign(s), \end{aligned} \quad (11)$$

where k_i, eta_i are positive constants. Taking derivative of the sliding surface (10) and substituting control law (11) give the approach law of the improved sliding mode manifold:

$$\begin{aligned} \dot{s} = & \frac{p}{\beta q}(e_{2i} - \hat{d}_i)^{p/q-1}[\ddot{x}_d - f(\nu) - \tau_M - \dot{\hat{d}}_i] \\ & + \dot{e}_{1i}(1 + e_{1i}^2)^{p/q-1}[1 + \frac{2p}{q}e_{1i}arctan(e_{1i})] \\ = & -\frac{p}{\beta q}(e_{2i} - \hat{d}_i)^{p/q-1}[k_i s + eta_i \cdot sign(s)] \\ & - (d_i - \hat{d}_i)(1 + e_{1i}^2)^{p/q-1}[1 + \frac{2p}{q}e_{1i}arctan(e_{1i})] \\ = & -\frac{p}{\beta q}(e_{2i} - \hat{d}_i)^{p/q-1}[k_i s + eta_i \cdot sign(s)] \\ & + \frac{\tilde{d}_i L}{\frac{p}{\beta q}(e_{2i} - \hat{d}_i)^{p/q-1}}, \end{aligned} \quad (12)$$

among them $\tilde{d}_i = d_i - \hat{d}_i$ is the estimation error, $L = [1 + e_{1i}^2]^{\frac{p}{q}-1}[1 + \frac{2p}{q}e_{1i}arctan(e_{1i})]$. Then, let $|eta_i| > |\frac{\tilde{d}_i L}{\frac{p}{\beta q}(e_{2i} - \hat{d}_i)^{p/q-1}}|$, consider a Lyapunov function:

$$V = \frac{s^2}{2}, \quad (13)$$

the derivative of V is given:

$$\begin{aligned} \dot{V} = & ss \\ = & -s \frac{p}{\beta q}(e_{2i} - \hat{d}_i)^{p/q-1}[k_i s + eta_i \cdot sign(s)] \\ & + \frac{\tilde{d}_i L}{\frac{p}{\beta q}(e_{2i} - \hat{d}_i)^{p/q-1}}] \\ \leq & -s \frac{p}{\beta q}(e_{2i} - \hat{d}_i)^{p/q-1}[k_i s + \gamma_i \cdot sign(s)] \\ \leq & 0, \end{aligned} \quad (14)$$

where $\gamma_i > 0$, the improved sliding mode manifold will converge to zero in a finite time. When the sliding mode manifold converges to zero, i.e. $s = 0$. Also, due to the finite

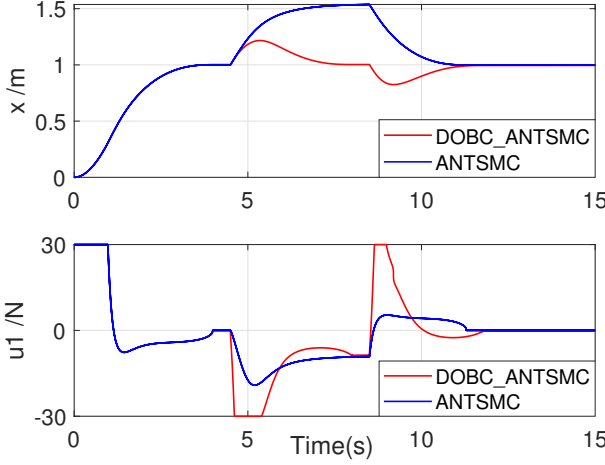


Fig. 3: The response curves of the position and control input under the DOBC framework and the ANTSMC without an observer respectively when the UBVMS is disturbed by a constant mismatched disturbance.

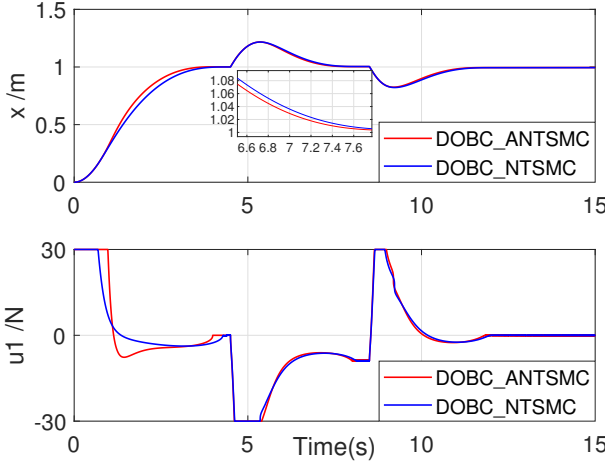


Fig. 4: The response curves of position and control input under two DOBC frameworks based on the ANTSMC and the NTSMC respectively when the UBVMS is disturbed by a mismatched constant disturbance.

time convergence of the disturbance observer, i.e. $\tilde{d}_i = 0$. It is derived from the (10) that the convergence time is:

$$t = \frac{p}{\beta^{q/p}(p-q)} \arctan^{1-q/p}[e_{1i}(t_f)], \quad (15)$$

where $e_{1i}(t_f)$ is the error between the actual system state and the desired system state. This implies that the system state can reach the desired state under the control of the improved DOBC method.

4 Simulations On an UBVMS

In this part, simulations are implemented to an UBVMS whose surge channel subjects to mismatched disturbances to verify our proposed DOBC method. The mass of the UBVMS is 45kg, and the parameters $\beta = 0.5, p = 5, q = 3, k_u = 7, eta_u = 0.5, \lambda_0 = 6, \lambda_1 = 4, \lambda_2 = 1$. Consider the initial system state (6) as $x_{1u} = 0m$, and the desired state $x_{1ud} = 1m$. A constant lumped mismatched disturbance $d_u = 0.5$ is imposed on the system from 4.5 seconds to 8.5 seconds.

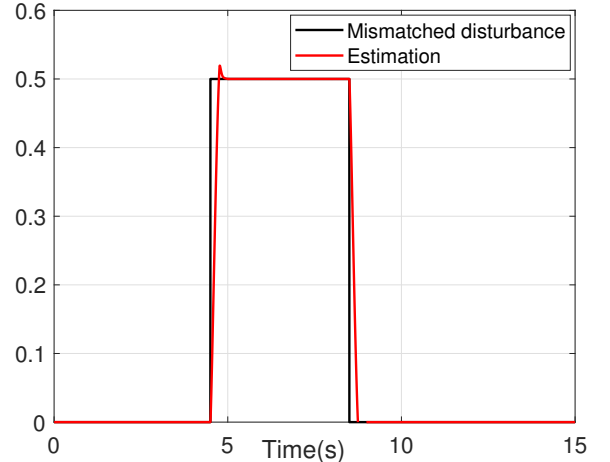


Fig. 5: Estimation performance of the observer for a constant mismatched disturbance.

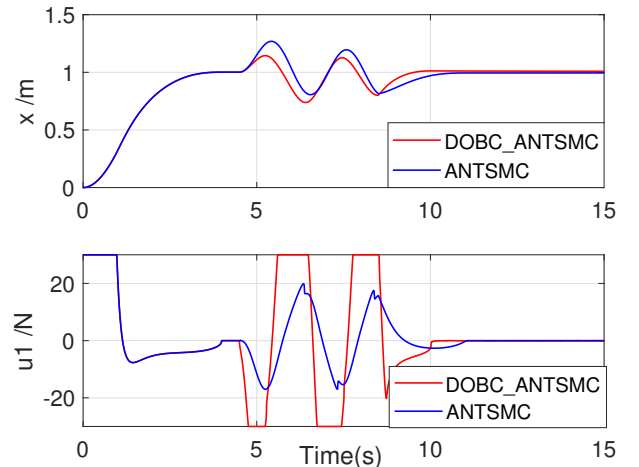


Fig. 6: The response curves under the DOBC framework and the ANTSMC only when the UBVMS is disturbed by a time-varying sinusoidal mismatched disturbance.

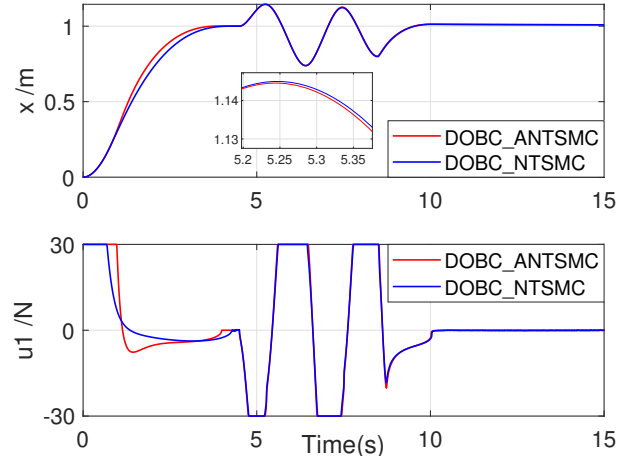


Fig. 7: The response curves under two DOBC frameworks when the UBVMS is disturbed by a time-varying sinusoidal mismatched disturbance.

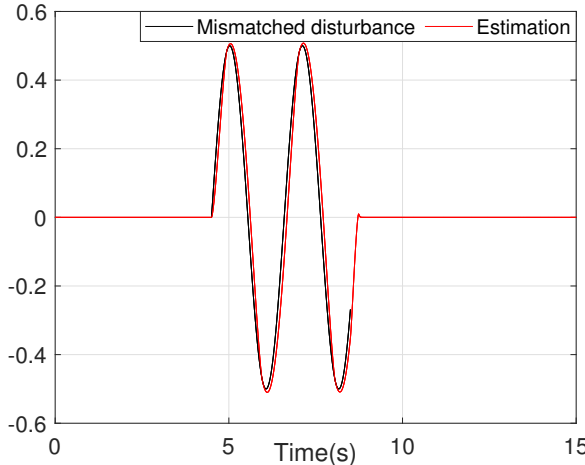


Fig. 8: Estimation performance of the observer for a time-varying sinusoidal disturbance.

Fig. 3 gives the position change curves and the control inputs of the DOBC method and the ANTSMC without an observer. The red line and the blue line in the first subgraph denote the position change under the DOBC based on the ANTSMC and the ANTSMC without observer respectively. It can be seen that the position change is smaller under the DOBC method than the ANTSMC only. And the ANTSMC cannot fully overcome the disturbance, the UB-VMS returns to the desired position unless the disturbance disappears or the magnitude is reduced. However, due to the finite time convergence of the observer, the proposed DOBC method based on the ANTSMC can track and compensate for the constant mismatched disturbance, and the UBVMS can return to the desired position under the influence of the mismatched disturbance at about 7 seconds, which is shown by the red line. The position change at about 9 seconds is caused by the immediate disappearance of the disturbance, but the UBVMS is affected by the non-zero control input, which makes it cannot maintain the current position instantly due to the inertia. The comparison of control inputs is displayed in the second subgraph, the control input generated by the DOBC method increases to offset the observed disturbance, while this phenomenon cannot be seen in the blue line.

Fig. 4 shows the comparison of the DOBC method based on the ANTSMC and the NTSMC respectively. As we can see, the DOBC based on the ANTSMC is better than NTSMC in system state convergence and disturbance resistance. And the calculated ANTSMC control input represented by the red line is a bit larger than the NTSMC represented by the blue line, which validates that the UBVMS can reach the desired position faster under the DOBC based on the ANTSMC. Fig. 5 shows the performance of disturbance observer on a constant disturbance tracking. The observer can track the constant disturbance in finite time.

As for time-vary mismatched disturbances, a sinusoidal disturbance with an amplitude of 0.5 is imposed on the UB-VMS. Fig. 6 shows the comparison between the ANTSMC with disturbance observer and non-disturbance observer. The DOBC method can reduce the influence of the time-vary mismatched disturbance, and the control input is larger

than the ANTSMC without an observer to alleviate the influence of the disturbance. Fig. 7 shows that the DOBC based on the ANTSMC can make the system state converge to the desired position faster, and the influence of the mismatched disturbance under the ANTSMC is smaller than under the NTSMC. Control inputs under both DOBC methods are given in the second subgraph. The larger calculated ANTSMC control input also validates the ANTSMC compensates for the time-vary disturbance more greatly. The observer tracks the time-vary mismatched disturbance shown in Fig. 8.

5 Conclusions

In response to the mismatched disturbances faced by the UBVMS, a DOBC framework composed of an ANTSMC and a finite time convergence disturbance observer is proposed. The stability of the system is validated by the Lyapunov theory. The simulations on an UBVMS affected by a constant mismatched disturbance and a time-vary mismatched disturbance validate the anti-mismatched disturbances performance of our proposed DOBC framework. Compared with the ANTSMC without an observer and the DOBC based on a NTSMC, the proposed DOBC based on the ANTSMC has a smaller position offset and faster convergence speed in the presence of the mismatched disturbances.

References

- [1] E. Simetti, F. Wanderlingh, S. Torelli, M. Bibuli, A. Odetti, G. Bruzzone, D. L. Rizzini, J. Aleotti, G. Palli, L. Moriello, and U. Scarcia. Autonomous underwater intervention: Experimental results of the maris project. *IEEE J. Ocean. Eng.*, 43(3):620–639, Jul. 2018.
- [2] G. Marani, S. K. Choi, and J. Yuh. Underwater autonomous manipulation for intervention missions auvs. *Ocean. Eng.*, 36(1):15–23, Jan. 2009.
- [3] P. Cieslak, P. Ridao, and M. Giergel. Autonomous underwater panel operation by girona500 uvms: A practical approach to autonomous underwater manipulation. In *Proc. IEEE Int. Conf. Robot. Autom.*, Seattle, WA, USA, May 2015: 529–536.
- [4] H. Nakajoh, T. Miyazaki, T. Sawa, F. Sugimoto, and T. Murashima. Development of 7000m work class rov “kaiko mk-iv”. In *Proc. OCEANS 2016 MTS/IEEE Monterey*, Monterey, CA, USA, Sep. 2016: 1–6.
- [5] G. Casalino *et al.* Underwater intervention robotics: An outline of the italian national project maris. *J. Mar. Technol. Soc.*, 50(4):98–107, Jul. 2016.
- [6] S. Zhang, Y. Qian, P. Liao, F. Qin, and J. Yang. Design and control of an agile robotic fish with integrative biomimetic mechanisms. *IEEE/ASME Trans. Mechatronics*, 21(4):1846–1857, Aug. 2016.
- [7] X. Li, Q. Ren, and J. Xu. Precise speed tracking control of a robotic fish via iterative learning control. *IEEE Trans. Ind. Electron.*, 63(4):2221–2228, Apr. 2016.
- [8] T. Salumäe, A. Chemori, and M. Kruusmaa. Motion control of a hovering biomimetic four-fin underwater robot. *IEEE J. Ocean. Eng.*, 44(1):54–71, Jan. 2019.
- [9] R. Wang, S. Wang, Y. Wang, M. Tan, and J. Yu. A paradigm for path following control of a ribbon-fin propelled biomimetic underwater vehicle. *IEEE Trans. Syst., Man, Cybern., Syst.*, 49(3):482–493, Mar. 2019.
- [10] D. Ginoya, P. D. Shendge, and S. B. Phadke. Sliding mode control for mismatched uncertain systems using an extended disturbance observer. *IEEE Trans. Ind. Electron.*, 61(4):1983–1992, Apr. 2014.

- [11] J. Zhang, X. Liu, Y. Xia, Z. Zuo, and Y. Wang. Disturbance observer-based integral sliding-mode control for systems with mismatched disturbances. *IEEE Trans. Ind. Electron.*, 63(11):7040–7048, Nov. 2016.
- [12] J. Huang, S. Ri, T. Fukuda, and Y. Wang. A disturbance observer based sliding mode control for a class of underactuated robotic system with mismatched uncertainties. *IEEE Trans. Automat. Contr.*, 64(6):2480–2487, Jun. 2019.
- [13] H. Min, S. Xu, B. Zhang, and N. Duan. Practically finite-time control for nonlinear systems with mismatching conditions and application to a robot system. *IEEE Trans. Syst., Man, Cybern., Syst.*, 50(2):480–489, Feb. 2020.
- [14] J. Yang, J. Su, S. Li, and X. Yu. High-order mismatched disturbance compensation for motion control systems via a continuous dynamic sliding-mode approach. *IEEE Trans. Ind. Inform.*, 10(1):604–614, Feb. 2014.
- [15] N. Fischer, D. Hughes, P. Walters, E. M. Schwartz, and W. E. Dixon. Nonlinear rise-based control of an autonomous underwater vehicle. *IEEE Trans. Robot.*, 30(4):845–852, Aug. 2014.
- [16] Y. B. Shtessel, I. A. Shkolnikov, and A. Levant. Smooth second-order sliding modes: Missile guidance application. *Automatica*, 43(8):1470–1476, Aug. 2007.